JOURNAL OF MATERIALS SCIENCE: MATERIALS IN ELECTRONICS 7 (1996) 437–445

Effect of dispersion state of SnO_2 particles in a glass matrix on the densification behaviour and the electrical properties of SnO_2–glass composites

H. SHIOMI, H. KOBAYASHI, T. KIMURA, M. NAKAMURA
Department of Chemistry and Materials Technology, Faculty of Engineering and Design, Kyoto Institute of Technology, Matsugasaki, Sakyo-ku, Kyoto-shi, Kyoto 606, Japan

The present work was undertaken as part of a study to clarify the relationship between the electrical properties and the microstructure of the SnO_2–glass composite. The glass composites with different particle dispersions of SnO_2 were prepared under various mixing conditions of the starting powder. The densification behaviour and the electrical properties of the glass composites were discussed from quantitative analysis of the dispersion of SnO_2 particles in glass matrices. As a result, the glass composite having homogeneous particle dispersion densified and showed an abrupt increase in conductivity (κ) and the temperature coefficient of resistance (TCR) at a low firing temperature. But after the completion of densification, the glass composite with the inhomogeneous dispersion of SnO_2 particles showed a high κ and a TCR close to zero because the highly aggregated SnO_2 particles connect with each other to form highly electrically conductive networks.

1. Introduction

Glass composite materials containing a dispersion of fine semiconductive particles in a glass matrix have been put to some practical use for electronic parts such as IC thick film resistors. These materials offer a wide variety of possibilities for electrical use in the near future [1].

Glass composites containing the conductive particles RuO_2, $Pb_2Ru_2O_6$ and $Bi_2Ru_2O_7$ – particles with metallic properties – have been applied to thick film resistors. Many researchers are studying the relationship between microstructure and electrical properties of glass composites. Consequently, many experimental results have been reported on the effects of the material and process parameters on the electrical properties of the glass composites [2–6]. These studies consider parameters such as the particle sizes of the glass frit and the conductive component, and the conditions at mixing and firing. They suggest that the electrical properties of the glass composites are largely influenced by the microstructure, especially the dispersion of semiconductive particles in glass matrices. Hence, quantitative evaluation of the microstructure is quite desirable for the precise control of the electrical properties of the glass composites. But it is often usual for microstructural evaluation to be carried out qualitatively using a microscope. Up to now, few papers have discussed the electrical properties quantitatively from a microstructural point of view [7–9].

The standard Ru-based resistors are usually fired in an air atmosphere because they are compatible with precious metal terminations. But Cu conductors are now receiving attention to meet the demand for more densely packed components. Compared with precious metal conductors, Cu conductors have several advantages in electronic circuits, e.g. low electrical resistance, high resistance to solder leaching and to electromigration, and high cost performance [1]. But because the Cu conductors should be fired in N_2 atmosphere, to prevent oxidation of Cu metal, the standard Ru-based resistors cannot be used. In high-temperature N_2 atmospheres there is reduction of the conductive constituents and the components of the matrix glass. Therefore, the industry requires urgent development of new nitrogen-fireable thick film resistors which are compatible with the Cu terminations. For this purpose, various thick film resistors have been developed using many kinds of material as conductive components, for example, LaB_6, ZrB_2, TaN, $MoSi_2$, $TaSi_2$ [10, 11]. But many problems remain unsolved and these new materials are not yet in general use.

Semiconductive SnO_2, the focus of this study, is quite a stable *n*-type semiconductor and widely used in gas sensors. Besides these applications, semiconductive SnO_2 particles have been used industrially as electrically conductive components of the semiconductive glaze of a high-tension insulator at extremely high voltages [12]. Using semiconductive SnO_2 particles, this glaze is generally recognized to have more excellent electrical properties and electrochemical durability than glazes using other semiconductive

0957–4522

oxides, such as Fe_2O_3, TiO_2, NiO [13]. Moreover, SnO_2 has a higher themodynamic stability than RuO_2 in high-temperature N_2 atmospheres. Therefore, recent attempts have applied semiconductive SnO_2 particles, doped with Sb, to conductive components of the nitrogen-fireable thick film resistor [14], and some makers have shipped samples made on an experimental basis. But fundamental studies on the suitability of SnO_2–glass composites for thick film resistors have begun so recently that, compared with Ru oxide-glass composites, insufficient technological information is available for practical industrial applications.

The present study was undertaken to clarify the relationship between the change in the electrical properties and the microstructural development in the SnO_2–glass composite during firing. Glass composites having a different degree of SnO_2 particle dispersion were prepared under various mixing conditions. The firing temperature dependence of the densification behaviour and the electrical properties of the glass composites is discussed following quantitative analysis of the particle dispersion of SnO_2 in a glass matrix by computer-assisted image analysis on SEM photographs.

In our previous studies, it has been found that the electrical properties and the densification behaviour of thick film samples experience a large influence from the substrate [14]. Thus, it is quite difficult to discuss only the effect of the particle dispersion of SnO_2 in the glass matrix. Therefore, this study employed block-shaped samples experiencing no influence from the substrate.

2. Experimental details

2.1. Materials

$SnCl_4$ and $SbCl_5$ in ethanol solution were used to get an SnO_2/Sb_2O_5 composition in a weight ratio of 95/5. A fixed amount of ammonia water was added to the ethanol solution to have a hydroxide precipitate of Sn and Sb through the reactions.

$$SnCl_4 + 4NH_4OH \rightarrow Sn(OH)_4 + 4NH_4Cl \quad (1)$$

$$SbCl_5 + 5NH_4OH \rightarrow Sb(OH)_5 + 5NH_4Cl \quad (2)$$

Each precipitate was dried for 5 days on a hotplate at 110 °C then calcined at 400 °C for 90 min in air to remove NH_4Cl in the above reactions. The calcined powder ground with an automatic mortar for 30 min was fired at the rate of 5 °C min^{-1} to 900 °C then kept for 10 min in air. The obtained semiconductive SnO_2 powder was used as a conductive component of glass composites.

The glass frit was prepared by ball-milling a glass block having the chemical composition: 30 wt% SiO_2, 20 wt% B_2O_3, 30 wt% BaO, 5 wt% Al_2O_3 and 15 wt% ZnO, for 48 h in ethanol.

2.2. Preparation and characterization of the glass composite

The semiconductive SnO_2 particles were mixed with the glass frit in an SnO_2/glass weight ratio of 7/3. The three mixing conditions shown in Table I were used to prepare samples having different particle dispersion of SnO_2 in glass matrices.

In order to characterize a degree of mixing, concentrations of Sn were measured with an energy dispersive X-ray spectroscope (EDX) using the SnL_α line on 20 randomly selected areas of 2.0 μm × 2.0 μm on the fractured surface of a powder compact. A homogeneity (H) of SnO_2 in the powder mixture was calculated by Equation 3 from the results of EDX analysis [15].

$$H = 1 - \frac{\sigma}{\sigma_0} \quad (3)$$

where σ, from Equation 4, is the standard deviation in the measured concentrations of Sn, and σ_0, from Equation 5, is the standard deviation when the mixed powders are assumed to be completely separated.

$$\sigma = \sqrt{\frac{\Sigma(X_i - a)^2}{N}} \quad (4)$$

$$\sigma_0 = \sqrt{a(1-a)} \quad (5)$$

where N, X_i and a represent, respectively, the number of the areas analysed ($N = 20$), a measured concentration of Sn in the ith area and an arithmetical average of X_i ($i = 1 \sim 20$).

The electrical conductivity (κ_m) of the powder mixture was measured under a uniaxial pressure of 130 MPa in order to infer the connectivity of SnO_2 particles in a powder compact before firing using the apparatus for measurement of the electrical conductivities of powder materials [16].

The powder mixtures were compacted uniaxially at 57 MPa into blocks of 1.0 cm × 1.0 cm × 0.5 cm before firing at various temperatures between 700 °C and 1100 °C for 10 min in air.

Ag electrodes were sputtered on to the opposite polished surfaces of specimens. A voltage drop between the electrodes was measured from 25 °C to 140 °C in dry N_2 gas flow under an electric current of 1 mA d.c. The electrical conductivity (κ) and the temperature coefficient of resistance (TCR) were calculated using Equations 6 and 7.

$$\kappa = \frac{IL}{VA} \quad (\Omega^{-1}\,cm^{-1}) \quad (6)$$

where I, L, V and A represent, respectively, an electric current flowing through the specimen, the thickness of the specimen, the voltage drop between the electrodes and the area of each electrode.

$$TCR = \frac{R_t - R_T}{R_T(t - T)} \times 10^6 \quad (p.p.m.\,{}^\circ C^{-1}) \quad (7)$$

TABLE I Mixing conditions of the starting powder

Sample	Mixing condition
A	Dry mixing with an automatic mortar for 45 min
B	Wet mixing with a ball mill for 3 h
C	Wet mixing with an attrition mill for 12 h

where R_t and R_T denote the electrical resistances measured at t °C and T °C, respectively. The present study used $t = 140$ °C and $T = 25$ °C.

Specimen porosity was calculated from bulk density and true density. Bulk densities were measured by Archimedes' method using water. True densities of oven-dried and finely ground samples were measured with a pycnometer employing the He gas displacement technique.

2.3. Microstructural characterization of the glass composite

Scanning electron microscope (SEM) observations were carried out on the fractured surfaces of the specimens fired at various temperatures. The dispersion state of SnO_2 particles in a glass matrix was observed with SEM after the fractured surfaces of the specimens were etched in 28% HF aqueous solution for 20 min to remove matrix glass phases. Then for the original SEM photograph of the etched specimen, image data from an area, 1.6 μm × 1.6 μm, was saved through a CCD camera to a personal computer and stored as co-ordinate data of 256 × 256 pixels. Using a digitizer, it was converted to an image with no tonal value (no shades). Fig. 1 shows an original SEM photograph and its digitized image. A ratio (S) was calculated as the area occupied by SnO_2 particles divided by the area of the image. A mean value of S was calculated for each specimen by looking at 60 images within its SEM photograph.

3. Results and discussion

3.1. Dispersion state of SnO_2 particles in the compacted powder mixture

Fig. 2 shows the SEM photographs taken over the fractured surfaces of compacted powder mixtures before firing. Sample A exhibits large glass particles and SnO_2 aggregates of almost equal size. Sample B exhibits large glass particles, but the SnO_2 aggregates are not as large as in sample A. This indicates that, during ball milling, the large SnO_2 aggregates are easily disintegrated into primary particles or smaller

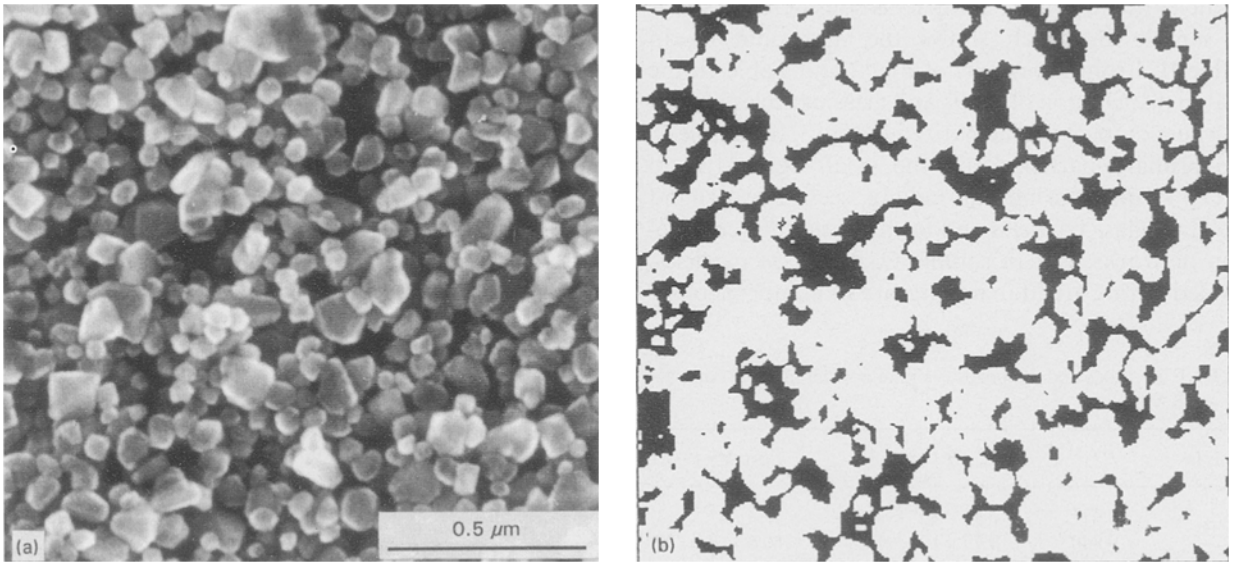

Figure 1 (a) An original SEM photograph taken after HF etching and (b) its digitized image used to calculate S = area occupied by SnO_2/area of digitized image. The specimen is sample C fired at 1100 °C.

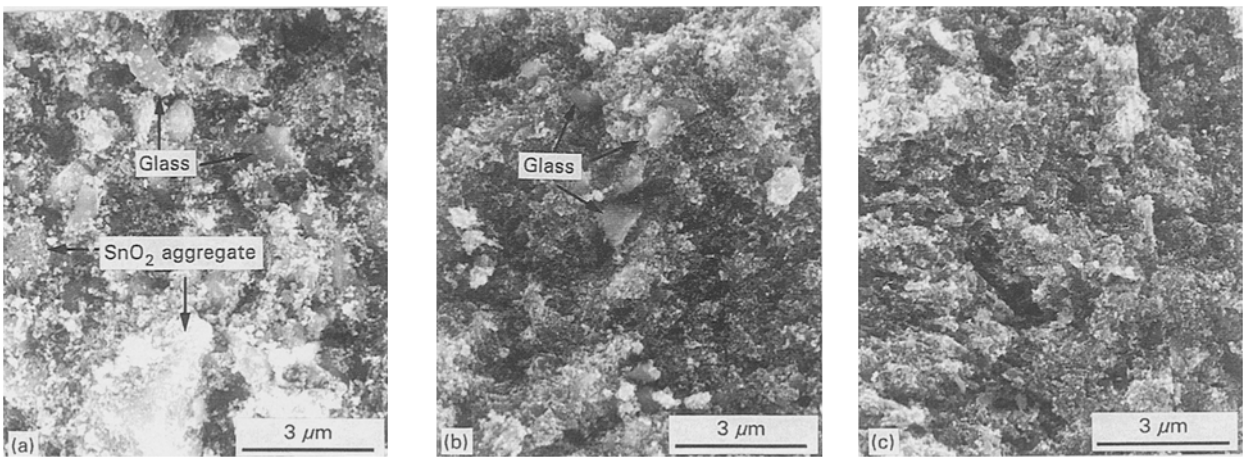

Figure 2 Comparison of the dispersion state of SnO_2 particles in the unfired powder compacts. (a) sample A, (b) sample B, (c) sample C.

aggregates. On the other hand, sample C exhibits neither large glass particles nor SnO_2 aggregates. From the above SEM observations, it appears that the particle dispersion in the compacted powder mixture is the most homogeneous in sample C and the most inhomogeneous in sample A.

The above experimental results agree well with the calculated values of H in Table II. In sample C, pulverization of the large glass particles probably occurs along with disintegration of the SnO_2 aggregates under the high shear stress during attrition milling. As a result, the homogeneous mixing of SnO_2 particles with glass frit is effectively attained in sample C. On the other hand, the dispersion of SnO_2 particles is inhomogeneous in sample A because the large glass particles and the SnO_2 aggregates are lightly ground with an automatic mortar (Fig. 2).

The electrical conductivities (κ_m) of the powder mixtures measured under a uniaxial loading of 130 MPa are also given in Table II; κ_m was minimum for sample C and maximum for sample B. The electrical conduction in the powder compacts probably develops through the direct touching paths of semiconductive SnO_2 particles. Hence, the best connectivity of SnO_2 particles in the powder compact is considered to occur in sample B, which shows the maximum κ_m in Table II. From the results of Fig. 2 and Table II, the spatial distribution of SnO_2 and glass particles in each powder compact is schematized in Fig. 3. In sample B, the primary particles and the small aggregates of SnO_2, formed during ball milling, seem to surround the large glass particles and form continuous conduction networks. But in sample C, fine glass particles, yielded during attrition milling, are so homogeneously distributed between particles of SnO_2 that the formation of the continuous conduction paths will be quite difficult. And the highly aggregated sample A shows poorer connectivity of SnO_2 particles than sample B.

TABLE II H, κ_m and the porosity of the powder mixture compacted at 58 MPa

Sample	H[a]	κ_m (Ω^{-1} cm^{-1})[b]	Porosity (%)
A	0.721	3.89×10^{-2}	48.3
B	0.840	9.77×10^{-2}	50.6
C	0.941	1.19×10^{-3}	52.9

[a] The homogeneity of SnO_2 particles in a glass matrix calculated by Equation 3.
[b] The electrical conductivity of the powder mixture measured at a uniaxial loading of 130 MPa.

3.2. Densification behaviour of the glass composite

Figs 4 and 5 show the changes in the linear shrinkage and the porosity of the glass composite with firing temperature. Fig. 6 shows the SEM observation results of the fractured surfaces of the specimens fired at various temperatures.

Figs 4 and 5 show that sample C densifies at a lower firing temperature than samples A and B. The principal reason for the enhancement of the densification in sample C at a low firing temperature must be the increase in the sinterability of glass particles caused by the high pulverization of large glass particles during attrition milling [17]. That is, the densification in sample C, due to the sintering and the coalescence of fine glass particles, occurs more efficiently than in samples A and B, even at low firing temperatures. Besides, at low firing temperatures, the densification in sample B is poorer than in sample A, although the glass particles are almost the same size in both samples, as seen in Fig. 2. In sample B, glass particles do not make contact with each other because they are homogeneously covered with SnO_2 particles, as shown in Fig. 3. So in sample B it is probably difficult for densification to proceed at low firing temperatures, due to the sintering of glass particles.

As seen from Fig. 6, denser areas are formed when, at 800 °C, molten glass penetrates the intraparticle voids of SnO_2 aggregates. Then they link with each other and surround pores. These dense areas coalesce by the viscous flow of glass as the firing temperature is increased. Further increase in firing temperature causes SnO_2 particles to approach each other under the capillary force arising from the layer of molten glass between SnO_2 particles. At the same time, the glass melt between SnO_2 particles may be squeezed out to the pores surrounded by the dense areas, further decreasing the porosity of the specimens. Moreover, it is evident from Fig. 6 that the pores and their surrounding dense areas are smaller in the sample

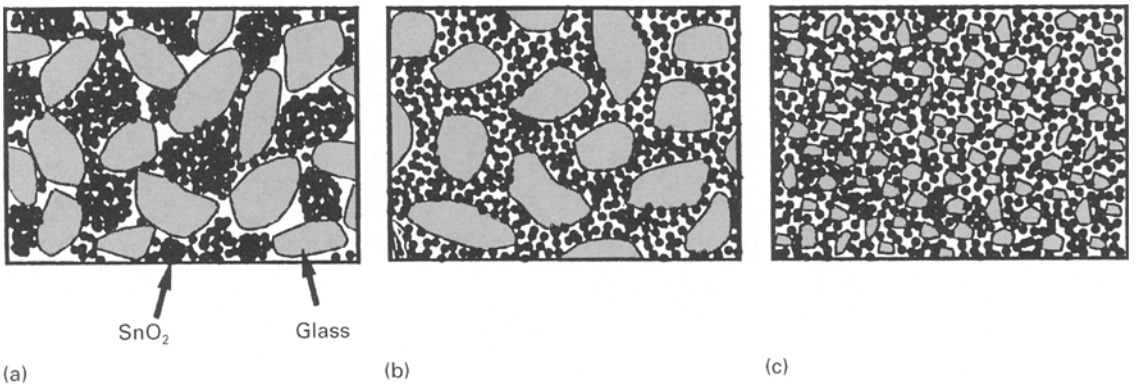

Figure 3 Schematic presentation of the spatial distribution patterns of SnO_2 and glass particles in the powder compacts: (a) sample A, (b) sample B, (c) sample C.

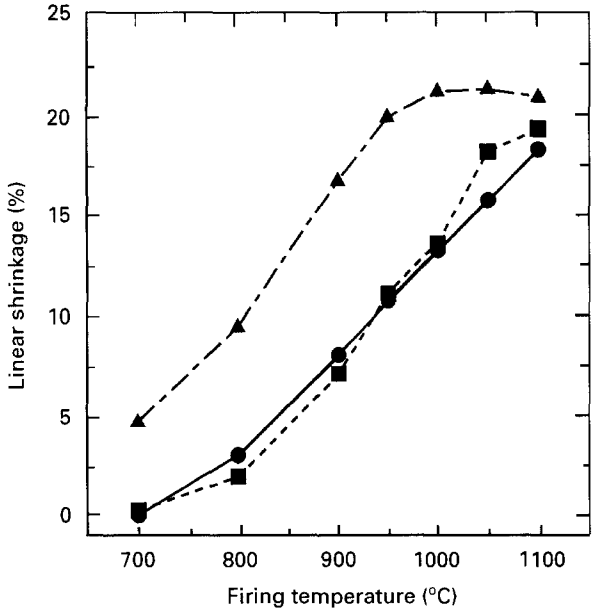

Figure 4 Change in linear shrinkage of the glass composite with firing temperature: (●) sample A, (■) sample B, (▲) sample C.

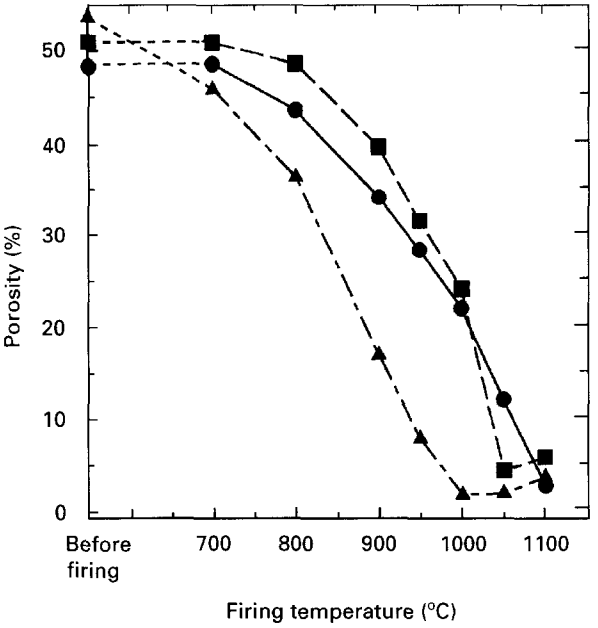

Figure 5 Change in porosity of the glass composite with firing temperature: (●) sample A, (■) sample B, (▲) sample C.

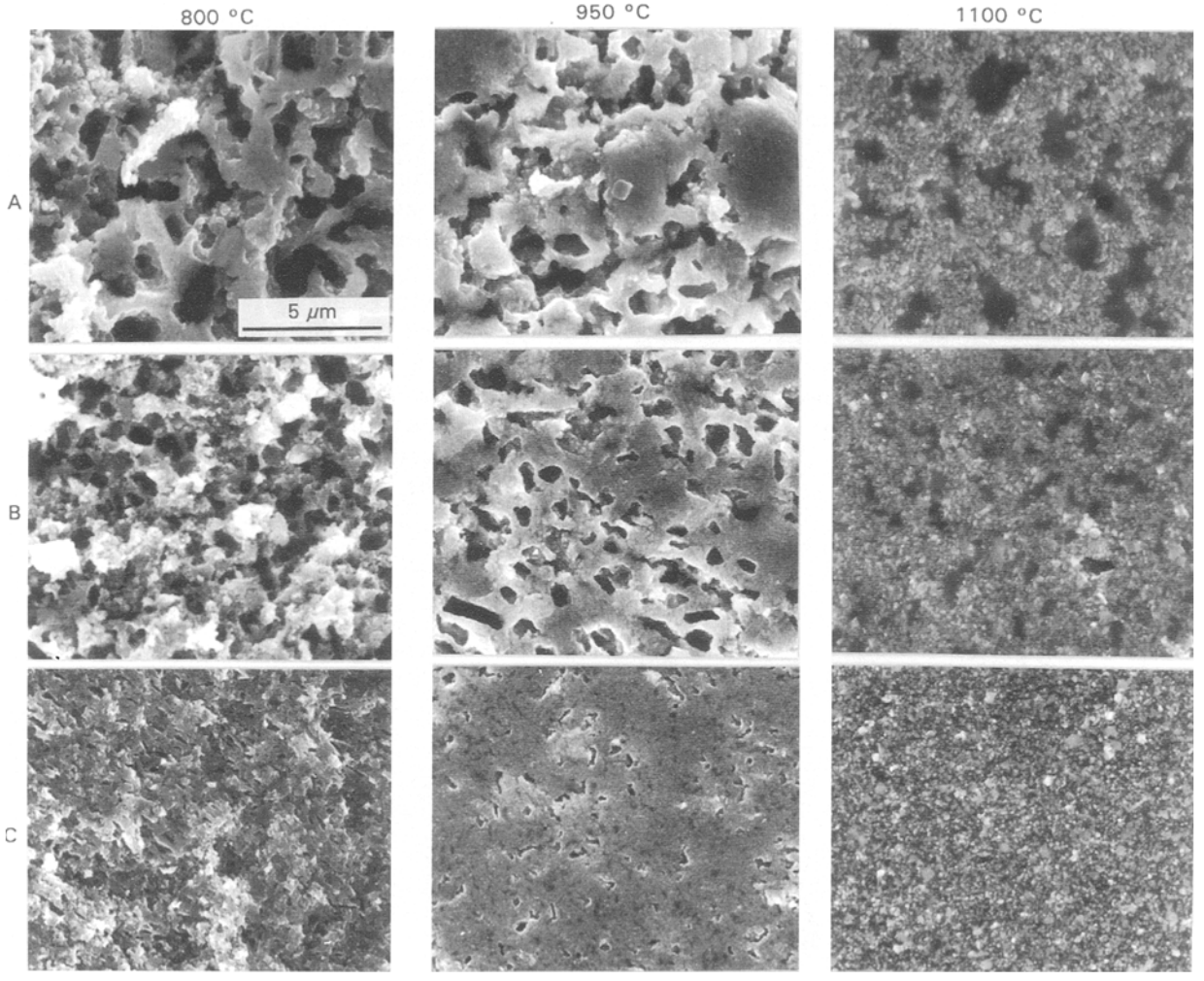

Figure 6 Comparison of microstructure development with firing temperature for samples A, B and C. The scale bar applies to all nine photographs.

having a more homogeneous dispersion of SnO_2 particles. The dense areas separated by the small pores will easily coalesce with each other. Therefore, the degree of densification in sample C, which has the most homogeneous dispersion of SnO_2 particles, is larger than in samples A and B, as shown in Figs 4 and 5. And from Fig. 6, the homogeneous dispersion of SnO_2 particles in sample C is still present once the

specimen has fully densified. But in samples A and B, the aggregates of SnO_2 remain to form network structures, even at 1100 °C firing.

In summary, the densification in the present system may proceed through the following steps: (1) the sintering and coalescence of glass particles, (2) the formation of dense areas due to the penetration of molten glass into SnO_2 aggregates, (3) the coalescence of the dense areas by viscous flow of glass, (4) the elimination of pores by effusion of molten glass from between SnO_2 particles into the pores. Furthermore, the densification behaviour is considerably influenced by the particle size of the glass frit and the uniformity of mixing of the starting powder.

3.3. Dependence of the electrical conductivity on firing temperature

The electrical conductivity (κ) of the glass composites measured at 25 °C is expressed in Fig. 7 as a function of firing temperature. It is found that κ for all samples decreases with increasing firing temperature up to 900 °C. But in sample C the decrease in κ with firing temperature is smaller than in samples A and B. At 700 °C firing, the melting of large glass particles is insufficient in samples A and B, so there is no change in the conduction paths formed when SnO_2 particles make contact with each other. Hence, κ is high for samples A and B when fired at 700 °C. However, the penetration of molten glass into the contact points between SnO_2 particles decreases the connectivity of the conduction paths. Therefore, κ for samples A and B decreases with increasing firing temperature. Similarly, the connectivity of the conduction paths in sample C probably decreases due to the penetration of glass between SnO_2 particles. The continuity between the conduction paths simultaneously increases because of the enhanced densification shown in Figs 4 and 5; this compensates for the decrease in κ due to the penetration of glass between SnO_2 particles.

In all samples fired above 900 °C, κ increases with firing temperature. And κ for the sample having the more homogeneous particle dispersion of SnO_2 increases significantly at lower firing temperatures. Moreover, κ increases with an increase in the average value of S, as shown in Fig. 8. It is evident from Fig. 9 that the average value of S increases with decreasing porosity. Judging from Fig. 9, the increase in S with increasing firing temperature in Figs 10 and 11 suggests that the highly populated areas of SnO_2 particles approach each other during densification. An increase in the areas of larger S will cause the highly conductive paths to form by mutual connections of SnO_2 particles or by the highly conductive solution layers around SnO_2 particles [18]. Hence, κ increases significantly with increasing S. When the dispersion of SnO_2 particles becomes more homogeneous, densification proceeds and, at lower firing temperatures, S increases significantly, as seen from Figs 5 and 9. Therefore, it is considered that κ for sample C, which has homogeneous dispersion of SnO_2 particles, largely increases at low firing temperatures.

Fig. 12 shows the relationship between the κ of the glass composite at 25 °C and the coefficient of variation (CV) of S, defined as a width of the S distribution. From Fig. 12 it is found that the densely sintered specimens having the larger CV show the higher κ. Apparently, from Fig. 11, with increasing firing temperature, the average value of S increases and CV decreases. However, the CVs of samples A and B are still larger than the CV of sample C even at 1100 °C. This indicates that SnO_2 aggregates are still present in samples A and B when fired at 1100 °C. Also, it is found from Fig. 6 that the SnO_2 aggregates can form network structures in samples A and B. In these networks, SnO_2 particles are quite close to neighbours, therefore, highly conductive paths will be formed. Moreover, the SnO_2 networks are thicker in the

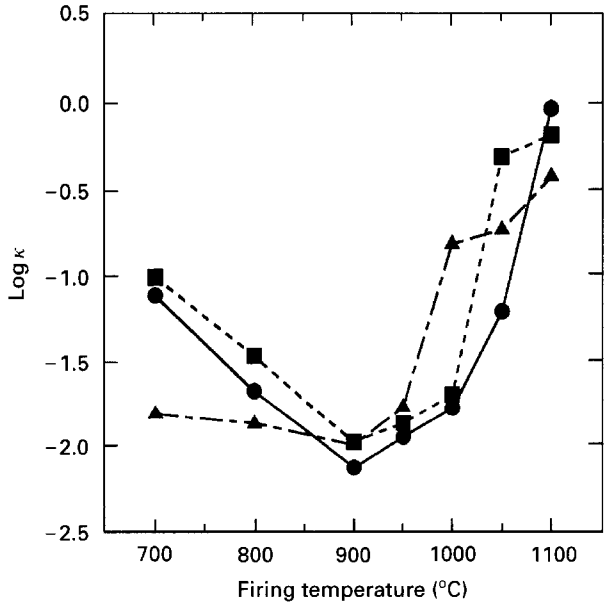

Figure 7 Change in electrical conductivity (κ) of the glass composite measured at 25 °C with firing temperature: (●) sample A, (■) sample B, (▲) sample C.

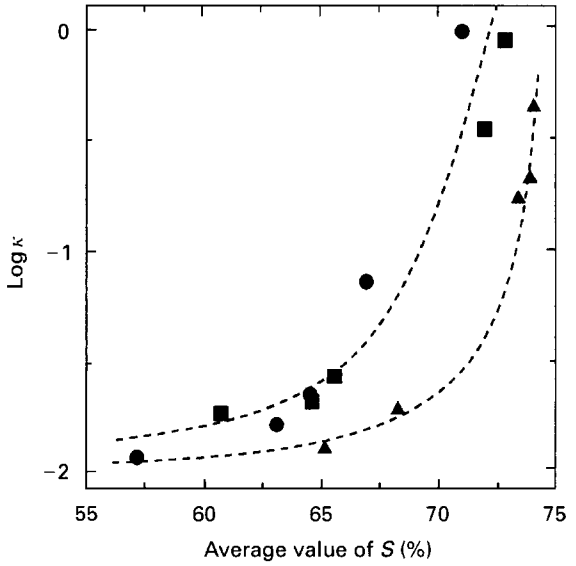

Figure 8 Relationship between the average value of S and κ of the glass composite measured at 25 C: (●) sample A, (■) sample B, (▲) sample C.

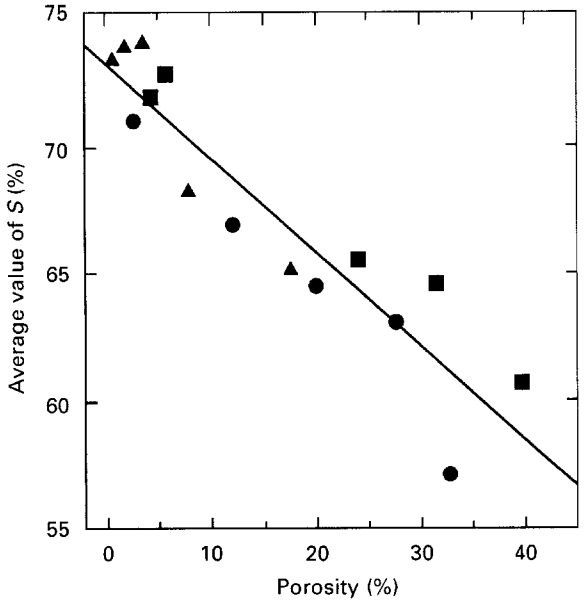

Figure 9 Relationship between the average value of S and the porosity of the glass composite: (●) sample A, (■) sample B, (▲) sample C

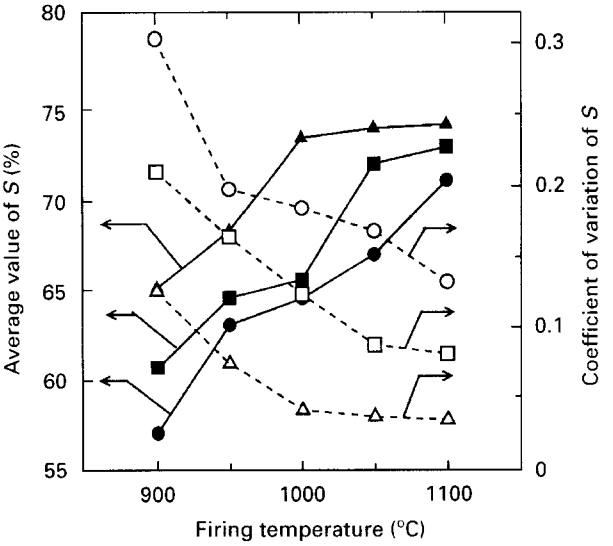

Figure 11 Changes in the average value of S (filled symbols) and the coefficient of variation (CV) of S (open symbols) with firing temperature: (●, ○) sample A, (■, □) sample B, (▲, △) sample C. CV is the width of the distribution of S values

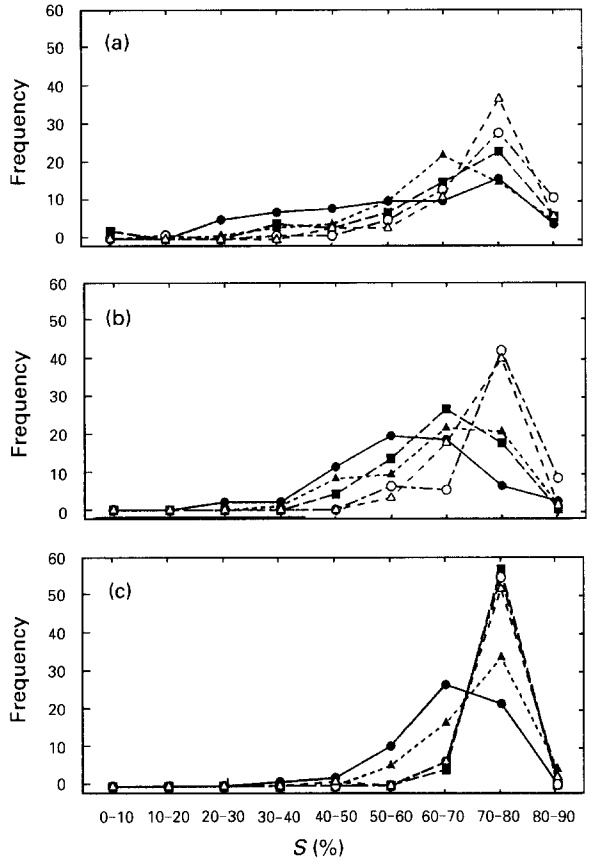

Figure 10 Change in the distribution of S with firing temperature (a) sample A, (b) sample B, (c) sample C. Key to firing temperatures (°C):(●) 900, (▲) 950, (■) 1000, (○) 1050, (△) 1100

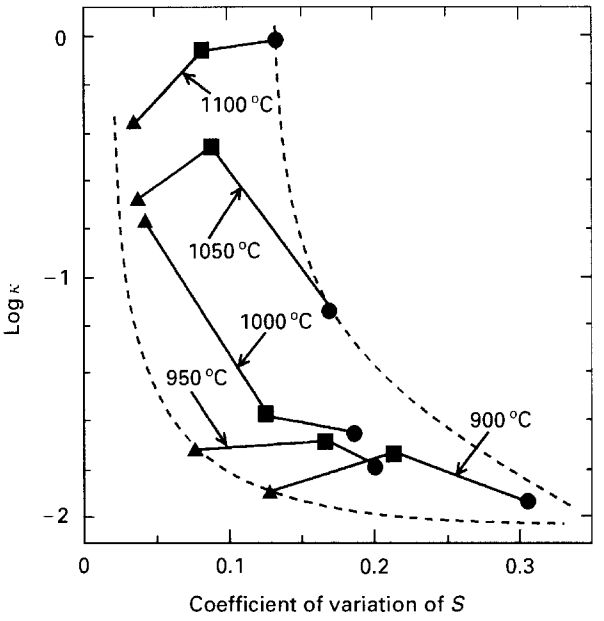

Figure 12 Relationship between CV and κ of the glass composite measured at 25 °C: (●) sample A, (■) sample B, (▲) sample C

sample having the larger CV. As a result, sample A fired at 1100 °C has the largest CV and shows the highest κ. On the other hand, SnO_2 particles are so homogeneously dispersed in sample C, which has the largest S and the smallest CV, that the matrix glass uniformly intervenes between SnO_2 particles. Thus, the distances between SnO_2 particles in the conduction paths of sample C will be larger than in samples A and B. Consequently, κ for sample C is lower than for samples A and B.

3.4. Dependence of TCR on firing temperature

Fig. 13 shows the dependence of the temperature coefficient of resistance (TCR) on firing temperature for samples A, B and C. Comparing Fig. 13 with Fig. 7, it is found that the highly conductive specimens fired at low temperatures show TCRs close to zero. Also, TCR decreases when κ decreases with increasing firing temperature. As described in the last section, electrical

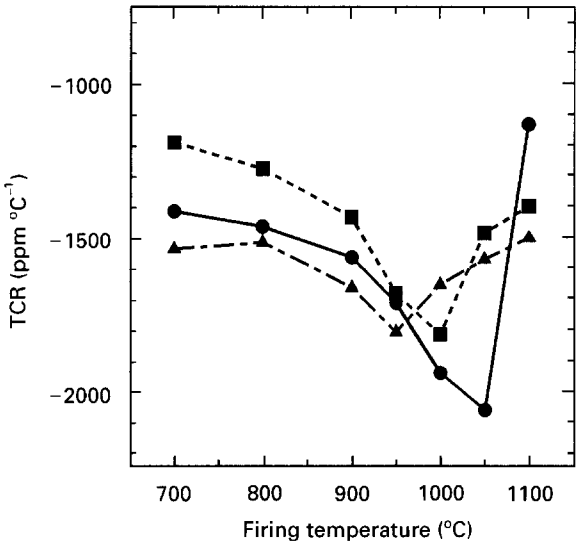

Figure 13 Change in temperature coefficient of resistance (TCR) of the glass composite with firing temperature: (●) sample A, (■) sample B, (▲) sample C.

conduction in the specimen fired at low temperatures occurs through the paths formed by the mutual connections of SnO_2 particles. Thus, the resistance of the conduction path consists of the volume resistance of each SnO_2 particle and the contact resistance between SnO_2 particles. And a compressive stress acts between SnO_2 particles below the strain point of matrix glass; this is due to the difference between the thermal expansion coefficients of SnO_2 ($20.1 \times 10^{-7}\,°C^{-1}$) and the matrix glass ($60.1 \times 10^{-7}\,°C^{-1}$). This compressive stress decreases on heating because of the larger thermal expansion of the matrix glass, increasing the contact resistance between SnO_2 particles. On the other hand, the volume resistance of each SnO_2 particle decreases on heating. Therefore, the change in the resistance of the conduction paths on heating will become small. So TCR for specimens fired at low temperatures becomes close to zero.

The penetration of glass between SnO_2 particles at an elevated firing temperature causes the resistance of the conduction paths of SnO_2 particles to increase. At the same time, TCRs for the conduction paths probably become more negative because of the intervention of glass with a large negative TCR between SnO_2 particles. Consequently, specimen TCRs decrease with increasing firing temperature.

Above 900 °C, TCRs of all samples continue to decrease with increasing firing temperature, although κ gradually increases. Judging from the increase in S as densification progresses, the number of conduction paths is expected to increase. However, the penetration of glass into the conduction paths presumably continues because there is a further decrease in the viscosity of glass with increasing firing temperature. Hence, the values of κ and TCR for the conduction paths will further decrease. The value of κ is determined by a competition between the number of conduction paths and their conductivity; the paths consist of SnO_2 particles and glass phases. Therefore, in terms of this competition, the gradual increase in κ above 900 °C may be ascribed to the larger increase in the number of conduction paths due to densification. On the other hand, the specimen TCR may be dominated by the TCRs for the conduction paths, not by the number of the conduction paths. Therefore, the specimen TCR decreases with increasing firing temperature.

When the firing temperature increases, specimen TCRs abruptly increase with κ. In this case, the thermal expansion of the matrix glass will have a large influence on specimen TCRs. In the densely sintered specimens, SnO_2 particles are close to each other and form continuous conduction paths. When the matrix glass expands on heating, there is an increase in the distances between SnO_2 particles in the conduction paths. Hence, the resistance of the conduction paths tends to decrease on heating. On the other hand, SnO_2 particles forming the conduction paths have a negative TCR. These two opposing effects will therefore make the specimen TCRs close to zero. As described earlier, the aggregated SnO_2 particles form highly conductive networks in samples A and B. Therefore, the resistance of the conduction paths in both samples is much lower than in sample C because of the shorter distances between SnO_2 particles. However, the rate of increase in the resistance of the conduction paths caused by the thermal expansion of the matrix glass will be larger than in sample C. Consequently, TCRs for samples A and B become closer to zero than for sample C.

4. Summary

The SnO_2–glass composites with different particle dispersion have been prepared under various mixing conditions of the starting powder. The densification behaviour and the electrical properties of the glass composites were discussed from quantitative analysis of the dispersion of SnO_2 particles in glass matrices. The results obtained are summarized as follows:

(1) At low firing temperatures, κ and TCR for the glass composite decrease with increasing firing temperature. Both effects are attributed to the disconnection of the conduction paths of SnO_2 particles due to the penetration of glass between SnO_2 particles forming the conduction paths. At higher firing temperatures, the SnO_2 interparticle spacings decrease with densification, therefore, highly conductive paths will be formed, causing κ and TCR to increase with increasing firing temperature.

(2) The glass composite that has the more homogeneous particle dispersion densifies and shows a significant increase in κ and TCR at lower firing temperatures. But when comparing the densely sintered samples, κ becomes higher and TCR approaches zero when the highly aggregated SnO_2 particles form networks in the glass matrix.

From the above experimental results, it is suggested that the electrical conduction in the present system will develop selectively through the limited conduction paths being formed by the mutual connections of SnO_2 particles or the quite highly populated areas of

SnO_2 particles. Thus, the electrical properties of the glass composites largely depend on the degree of densification, the uniformity of the dispersion of SnO_2 particles in the glass matrix and therefore the distances between SnO_2 particles. Consequently, κ for the glass composite can be controlled by the spatial distribution of SnO_2 particles in the glass matrix. However, a constant TCR over a wide range of κ cannot be achieved only by controlling the particle dispersion of SnO_2 in the glass matrix. This is because the TCR of the glass composite varies according to κ, as mentioned above. Detailed investigation of other factors, such as thermal expansion coefficient of the matrix glass, may lead to the desired outcome–control that achieves constant TCR, independent of κ.

Acknowledgement

This research was financially supported in part by a research grant for 1994 from the Hosokawa Powder Technology Foundation.

References

1 MICROELECTRONICS SOCIETY OF JAPAN, in "IC-Thick Film Technology", edited by M Haradome, (Kogyo Chosakai, Tokyo, 1984) p 1
2. A. H BOONSTRA and C A H A MUTSAERS, *Thin Solid Films* **67** (1981) 13.
3. P F CARCIA, A FERRETTI and A SUNA, *J Appl. Phys* **53** (1982) 5282
4 T INOKUMA, Y TAKETA and M HARADOME, *IEEE Trans. Compon Hybrids Manuf. Technol* **CHMT-7** (1984) 166.
5. *Idem, ibid.* **CHMT-8** (1985) 372.
6. T YAMAGUCHI and K IIZUKA, *J Amer. Ceram. Soc* **73** (1990) 1953.
7. J V BIGGERS, J R McKELVY and W A SCHULZE, *ibid.* **65** (1982) C13.
8. S M CHITALE and R W VEST, *IEEE Trans. Compon Hybrids Manuf Technol.* **11** (1988) 604.
9. Y MIZUNO, T SHIMIZU, K TERASHITA and K MIYANAMI, *J. Soc Mater. Sci. Jpn* **42** (1993) 836.
10 H WATANABE and T ISHIDA, in Proceedings of the 5th International Microelectronics Conference, Tokyo, Japan (1988) p 37
11. T ISEKI, O MAKINO and K NISHIDA, in Proceedings of the 1989 ISHM, Baltimore, Maryland (1989) p. 168.
12. M NAKAMURA, H SHIOMI, S OKUDA and T NAGANO, *Yogyo-Kyokai-Shi* (*J Ceram Soc. Jpn*) **93** (1985) 170
13. D B BINNS, *Trans. Br. Ceram. Soc* **73** (1974) 1.
14. H SHIOMI, M NAKAMURA, Y MATSUMURA, K FUJIMURA, J ISHIGAME and K ONOUE, *J. Ceram. Soc. Jpn* **100** (1992) 634.
15. H E ROSE, *Trans Inst. Chem. Eng.* **37** (1959) 47
16. H SHIOMI, T FUKUZAKI and M NAKAMURA, *J Soc. Powder Technol Jpn* **30** (1992) 162.
17. W D KINGERY, H K BOWEN and D R UHLMANN, in "Introduction to Ceramics" (John Wiley, New York, 1960) p 490
18 M NAKAMURA, M KAMINO T NAGANO and M ARA KAWA, *Yogyo-Kyokai-Shi* (*J. Ceram. Soc. Jpn*) **95** (1987) 562.

Received 7 March
and accepted 5 July 1995